ZIBELINE INTERNATIONAL™ PUBLISHING

ISSN: 2521-0858 (Print)
ISSN: 2521-0866 (Online)
CODEN: SHJCAS

Science Heritage Journal (GWS)

DOI: http://doi.org/10.26480/gws.01.2026.19.26

RESEARCH ARTICLE

THE ELECTROCHEMICAL AND GRAVIMETRIC EFFECTS OPTIMIZATION OF CARICA PAPAYA LEAF CONSTITUENTS IN CORROSION INHIBITION

Ojike P. C., Ezeugo J.O., Ifediorah E. I.*

Department of Chemical Engineering, Chukwuemeka Odumegwu Ojukwu University, P.M.B. 6059. Anambra state, Nigeria.
Corresponding Author Email: ezekielifediorah@gmail.com

This is an open access article distributed under the Creative Commons Attribution License CC BY 4.0, which permits unrestricted use, distribution, and reproduction in any medium, provided the original work is properly cited.

ARTICLE DETAILS

Article History:

Received 26 January 2026
Revised 20 February 2026
Accepted 25 February 2026
Available online 4 March 2026

ABSTRACT

It was studied how the components of plant extracts affect corrosion inhibition both electrochemically and gravimetrically. There are growing concerns about the toxicity of conventional organic inhibitors; This has resulted in the study of plant-based, environmental alternatives for corrosion inhibition. This study has examined the electrochemical and gravimetric properties of the components of Carica papaya leaf extracts on the corrosion of mild steel, zinc, and aluminium using acidic HCl and H2SO4 as the media. The effectiveness of the inhibition was measured with the electrochemical impedance spectroscopy and gravimetric methods (response surface optimisation). The maximum efficiency of the extracts was between 75.42 and 84.56. EIS Nyquist diagrams demonstrated semicircles increasing with extract concentration which suggests an increase in Rct and decrease in capacitance that would be suitable to develop compact films whereas the gravimetric data represented that weight loss decreases in a dose-dependent fashion.Adsorption was Langmuir, Temkin, Frumkin, and Flory-Hoggins isotherms (R2 = 0.937-0.997) with relatively low Kads and delta Gads indicative of physisorptive electrostatic bonding. The study effectively verified that Carica papaya leaf is a viable, synergistic green inhibitor that is a suitable alternative for corrosion control.

KEYWORDS

Synergistic inhibition; Carica papaya; Gravimetric effects; RSM; Electrochemical analysis.

1. INTRODUCTION

Corrosion refers to electrochemical corrosion of metals and alloys, and is a considerable phenomenon in chemical engineering and industry, in which the world suffers annual losses of 2.5 trillion to 3-4% of the world GDP of materials, downtime, and environmental cleanup (Koch et al., 2019). The metals like aluminium (Al), mild steel (MS), and zinc (Zn) are anodically metal dissolved in the acidic environment, known as hydrogen of (H2), so as HCl and sulfuric acid (H2SO4), which are commonly used in acid pickling, in descaling, in treating of oil wells as well as in processing oil refineries. This not only reduces structural integrity but also perpetuates environmental risks, such as the leaching of heavy metals into effluents, in violation, for instance, of the The US EPA and European REACH regulations apply to harmful effluent limit (Verma et al., 2018). Efficiencies with respect to inhibition (IE%) can often be greater than 90percent via physisorption or chemisorption with the standard forms of corrosion inhibitors (primarily synthetic organic adjuvants such as imidazolines, phosphates and benzotriazoles) regulating these processes by sticking to the metal surface to form protective layers. Nevertheless, these issues have led to the increased demand of green inhibitors, suitable alternatives, non-toxic, and economically advanced green inhibitors derived out of natural sources, since they have chronic toxicity and low biodegradability, in addition to bioaccumulation in aquatic environments (Umoren and Solomon, 2019). The heteroatoms (N, O and S) enhance lone-pair donation as well as pi-electron coupling to the d-orbitals of the metal, creating compact films that are not sensitive to the environment. That is why plant extracts containing a significant amount of heterocyclic phytoconstituents are in the limelight such as alkaloids, flavonoids, phenols, and terpenoids (Dehghani et al., 2024).

Plant derived Inhibitors such as Carica papaya Leaf Extract (CPL) is notable as it is available, high yielding (12-18 wt% ethanol extraction) and has a rich metabolome, including quercetin (flavonoid, 45% abundance), caprine (alkaloid, 12%) and aliphatic hydrocarbons (C13-C20 n-alkanes, 25%), confirmed by gas chromatography-mass spectrometry (GC-MS) and Fourier Transform Infrared (FTIR) spectroscopy.31,32 These constituents allow for multifaceted inhibition: the presence of polar -OH/-COOH groups is responsible for electrostatically (physisorption, DeltaGads ca. -12 kJ/mol) and non-polar chains are responsible for hydrophobic shielding, which reduce the rate of corrosion (CR) by 80-90% in the acidic medium. Previous studies report up to 92% of CPL's IE% at MS in 15% HCl through mixed-type behaviour (PDP shifts <80 mV), that was attributed to Langmuir adsorption and increased charge transfer resistance (R_ct >400 O/cm2) in electrochemical impedance spectroscopy (EIS) (Rahim et al., 2023). Yet the optimisation of extract concentration, temperature, and immersion time to enable industrial-scale scalability remains a significant research gap, with integrated gravimetric-electrochemical correlations for multi-metal systems (Al, MS, Zn).

While numerous studies in the literature confirm the efficiency of plant extracts (e.g., 85-95% IE% for Vernonia amygdalina on Al by fatty acids; Vashi et al., 2025), there remain research gaps in overall optimisation. Response surface methodology (RSM) has simplified extraction yields, but it is rarely coupled with EIS for predictive IE% modelling ($R^2 > 0.95$). No study has measured electrochemical (EIS) and gravimetric (weight loss/RSM) parameters simultaneously.

This investigation addresses this gap by evaluating the electrochemical and gravimetric effects of CPL extracts on Al, MS, and Zn corrosion, with RSM-driven optimisation to maximise IE% performed. This work provides solid evidence of sustainable control of corrosion using CPL extracts as an acceptable bio-inhibitor.

Quick Response Code	Access this article online	
	Website: www.jscienceheritage.com	**DOI:** 10.26480/gws.01.2026.19.26

Cite The Article: Ojike P. C., Ezeugo J.O., Ifediorah E. I. (2026). The Electrochemical and Gravimetric Effects Optimization of Carica Papaya Leaf Constituents in Corrosion Inhibition. Science Heritage Journal, 10(1): 19-26.

2. Materials and Methods

2.1 Materials and Carica papaya leaf extract synthesis

Potentiostat/galvanostat 263 electrochemical work station, HCl solution, H 2 SO 4, analytical-grade acetone, mild steel, Emery paper, beaker, Philtre paper, thermometer, Shimadzu thermostatic bath FTIR spectrophotometer, Model IR affinity GCMS-QP2010 plus Shimadzu, Japan SEM (Model: Rhenom Prox, Phenom World Eindhoven, Netherlands).

The leaves to be used were Carica papaya collected in Okija and Ihembosi, in the Anambra state, Nigeria. During four days, the leaves were allowed to dry in the sun. The dried leaves were crushed into fine and stored in a tight container so as to cover a maximum area. Individual extractions involved weighing of 30 g of the crushed leaves and placing them in 1000cc of ethanol during a 48 hours period. All the combinations of the plants were filtered after 48 hours. The filtrate obtained is composed of a combination of plant extract and ethanol. The distilled solvent was then washed out and the concentrated extract of the ethanol solvent was harvested. In the case of corrosion inhibition study, the plant extract was weighed and stored.

Mild steel, aluminium and zinc coupon sheets were washed and polished using emery paper in order to arrive at a glossy polished surface. The coupons (from organic food) were washed by acetone, distilled water, dried out in the air and stored in the desiccators to eliminate organic contaminants (oil, etc.). Each of the coupons was accurately weighed on an electronic weighing scale and the initial weight was recorded.

2.2 Electrochemical Impedance Spectroscopy Measurements

To understand the characteristics and kinetics of electrochemical processes that occurred at the interface of the metal/solution, electrochemical impedance spectroscopy experiments were conducted to understand how they were changed by plant extracts. The frequency dispersion of the impedance data could be plotted using solid metal electrodes with the result usually being a depression of the Nyquist semicircle with the center below real axis.

It occurs due to the fact that the metal surface is irregular and coarse (Abdel-Gaber et al., 2009). To describe the transfer function a solution resistance, Rs, shorted by a capacitor C may be used in parallel with the charge transfer resistance, Rct.

$$Z_{(w)} = R_s + \left(\frac{1}{R_{ct}} + jwc\right)^{-1} \quad (1)$$

Nonetheless, this is a transfer property that cannot be used to describe the depression of the capacitive semicircle and that only applies to a homogeneous system with only a single time constant when the center of the semicircle lies on the abscissa. The non-ideal frequency response is replaced by a constant phase element (CPE) instead of the capacity. The application of such a CPE is related to surface inhomogeneities and it considers ideal dielectric behaviour departures. The CPE's impedance, Z, is:

$$Z_{CPE} = Q^{-1} (j^2w)^{-n} \quad (2)$$

and j 2 = i is an imaginary integer and Q and n are the CPE constant and exponent, respectively. Just as angular frequency (w = 2 -1 f, frequency Hz) can be expressed in radians (w = 2 -1 f), resistance (ZCPE = r, n = 0) and capacitance (ZCPE = C, n = 1) can be expressed in terms of CPE. This was compared with the impairment of the impedance spectra on an equivalent circuit model that had been utilized to explain the metal/acid interface in the past in order to determine the values of the respective parameters of the impedance (Oguzie et al., 2010; Chidiebere et al., 2015). The diameter of the Nyquist semicircle is correlated with charge transfer resistance (Rct). In both cases, addition of extract to the acid solution increased the size of Nyquist semicircle indicating that a corrosion process was blocked. Mechanism The strength of the process was not influenced by the concentration of plant extract but the higher the concentration of the plant extract, the higher the magnitude of the impedance response. Conversely, with the presence of the extract, the double-layer capacitance, or CdL fell and gradually declined with the increase in extract concentration. This decrease is usually caused either by the jacking up of the thickness of the two layers and/or reduction of the local dielectric constant. Extract species sticking to the contact of the metal/solution may explain the phenomenon. This would correspond to the Helm holtz which can be obtained in regard to the following equation:

$$C_{dL} = \frac{\varepsilon\varepsilon_0 A}{\delta} \quad (3)$$

Where ε 0 is the permittivity of free space and εr is the dielectric constant of the film. As a result, the trend in Cdl is that the increment of Rct might be explained by the fact that an adsorbed protective layer of the plant extract is formed at the interface of the metal and the solution which serves to protect the surface of the metal against corrosive action.

The efficiencies of the inhibitor (IE% at different concentration levels) of an inhibitor were calculated by drawing the Nyquist plot based on the following equation:

$$IE\% = \frac{R_{ct(inh)} - R_{ct}}{R_{ct(inh)}} x \frac{100}{1} \quad (4)$$

Where R_{ct} and $R_{ct(inh)}$ denotes charge transfer resistance in the absence and presence of the inhibitor.

2.3 Weight loss (gravimetric) method of the Corrosion Inhibition Study

The weight-loss method was undertaken in different temperatures and different levels of the plant extracts with one factor at a time. Mild steel coupons that had been weighed had each been placed in a 250 ml open beaker with an acid concentration. Also, metal coupons were placed in conducting open beakers (250 ml) having different acid concentrations and plant extract concentrations.

Periodically, weight loss was measured at various temperatures with and without extracts of varying concentration. The acetone was poured over the coupons at the right time and the coupons were cleaned using a running water with a bristle brush, dried and then their weight was again measured. The weight loss was calculated by the difference between the weight of the corrosion product at the beginning and the weight that was left after the removal of the corrosion product. Experiment readings were recorded. The weight loss (8), corrosion rate (CR) and the inhibition efficiency (IE) were calculated using equation (5), equation (6) and equation (7) respectively.

The surface coverage was determined by use of equation (8).

$$\Delta W = Wi - Wf \quad (5)$$

$$CR = \frac{W_i - W_f}{At} \quad (6)$$

$$IE\% = \frac{W_o - W_1}{W_o} \times 100 \quad (7)$$

$$\theta = \frac{W_o - W_1}{W_o} \quad (8)$$

In which, w1 and w o are the weight loss when the samples are added with the inhibitor and without an inhibitor, respectively, w i and w f are the initial and final weights of the mild steel samples. Entering the area, A, of the mild steel sample and the immersion period, t.

Response surface methodology (RSM) was used to analyse the reaction. Graphical and ANOVA analysis of the inhibition efficiencies were done. The coded factor and real factor mathematical model was obtained. The model was used to predict the response to given values of each element, in the context of coded factors. Factor levels that were high were given +1 and those that were low were denoted as -1. The optimal parameters of inhibition were discovered.

Table 1: Design matrix for the experiments

Std	Run	Factor 1, Acid Conc. (M)	Factor 2, Inhibitor Conc. (g/l)	Factor 3, Temperature (K)	Factor 4, Time (hr)	Response 1, Weight Loss (g)	Response 2, Corrosion Rate (mg/cm²hr)	Response 3, Inhibition Efficiency (%)
23	1	1	0.7	313	4	-	-	-
21	2	1	0.7	303	8	-	-	-
13	3	0.5	0.2	323	12	-	-	-
27	4	1	0.7	313	8	-	-	-

Table 1 (cont): Design matrix for the experiments								
29	5	1	0.7	313	8	-	-	-
7	6	0.5	1.2	323	4	-	-	-
4	7	1.5	1.2	303	4	-	-	-
6	8	1.5	0.2	323	4	-	-	-
3	9	0.5	1.2	303	4	-	-	-
30	10	1	0.7	313	8	-	-	-
22	11	1	0.7	323	8	-	-	-
9	12	0.5	0.2	303	12	-	-	-
14	13	1.5	0.2	323	12	-	-	-
10	14	1.5	0.2	303	12	-	-	-
19	15	1	0.2	313	8	-	-	-
1	16	0.5	0.2	303	4	-	-	-
16	17	1.5	1.2	323	12	-	-	-
11	18	0.5	1.2	303	12	-	-	-
24	19	1	0.7	313	12	-	-	-
2	20	1.5	0.2	303	4	-	-	-
25	21	1	0.7	313	8	-	-	-
20	22	1	1.2	313	8	-	-	-
26	23	1	0.7	313	8	-	-	-
17	24	0.5	0.7	313	8	-	-	-
8	25	1.5	1.2	323	4	-	-	-
15	26	0.5	1.2	323	12	-	-	-
12	27	1.5	1.2	303	12	-	-	-
18	28	1.5	0.7	313	8	-	-	-
5	29	0.5	0.2	323	4	-	-	-
28	30	1	0.7	313	8	-	-	-

3. Results and Discussions

3.1 Electrochemical Impedance Spectroscopy result of mild steel in the presence of CPL extract

Electrochemical impedance spectroscopy studies were conducted to value the nature and the kinetics of the electrochemical events in the interface of the metal/solution and the effect of the CPL extract on it. Fig. 1 has the Nyquist plot of the impedance response of mild steel at the presence of different CPL extract concentrations. In the high-frequency region, the resulting charts often just have a single depressed capacitive semicircle, and this is attributed to one time constant in the Bode plots. Frequency dispersion of the impedance data often occurs in solid metal electrodes indicating the observed depression of the Nyquist semicircle around the center not on the real axis. It takes place as a result of the irregularity and ruggedness of metal surfaces (Abdel Gaber et al., 2009). The transfer function may be represented by a solution resistance shorted by a capacitor C in parallel to the charge transfer resistance Rct:

$$Z_{(\omega)=} R_s + \left(\frac{1}{R_{ct}} + j\omega C\right)^{-1} \quad (9)$$

However, this transfer function cannot explain the depression of the capacitive semicircle and is only applicable to homogeneous systems with a single time constant when the semicircle's center is on the abscissa. A constant phase element is used in place of the capacitor when there is an undesirable frequency response (CPE). The use of such a CPE is associated with surface inhomogeneities and takes into consideration the departures from ideal dielectric behavior. The CPE's impedance, Z, is:

$$Z_{CPE} = Q^{-1}(j\omega)^{-n} \quad (10)$$

j2 = -1 is an imaginary integer and Q and n are the CPE constant and exponent respectively. With f as the frequency in Hz 2pi f = 2 omega and 2pi 2 = omega. CPE may represent either capacitance (ZCPE = C, n = 1) or resistance (ZCPE = R, n = 0). The generated impedance spectra were analysed using the parallel circuit model of an analogous circuit to determine the values of impedance parameters associated with the interface (Oguzie et al, 2010; Chidiebere et al, 2015). The diameter of the Nyquist semicircle is correlated with charge transfer resistance (Rct). The area of the Nyquist semicircle was greater in 1 M HCl as well as 0.5 M H2SO4 solution in the presence of CPL extract, indicating that corrosion process had been suppressed. The mechanism of the process was identical, but the higher concentration of CPL extract was, the larger was the impedance response. The Cdl decreased, on the other hand, in the presence of the extract and increased steadily with increasing PNL concentration. Such drop is usually due to the increase in the thickness of the double layer and/or reduction in the local dielectric constant. The behaviour may be due to adsorption of the PNL species at the metal/solution contact. This is in line with the Helmholtz model based on the equation.

$$C_{dl} = \frac{\varepsilon\varepsilon_o A}{\delta} \quad (11)$$

and ε0 is the relative permittivity of the film, and εo is that of the vacuum. The growth of adsorbed layer of CPL extract on the metal/solution interface, which protects the metal surface against corrosion, was the cause of the observed increase in Rct, as per the trend of Cdl.

The efficiency of inhibition (%IE) of different doses of inhibitors was calculated using the following formula according to the Nyquist plots:

$$IE\% = \left(\frac{R_{ct(inh)} - R_{ct}}{R_{ct(inh)}}\right) x\ 100 \quad (12)$$

Where R_{ct} and $R_{ct\ (inh)}$ denotes charge transfer resistance in the absence and presence of the inhibitor.

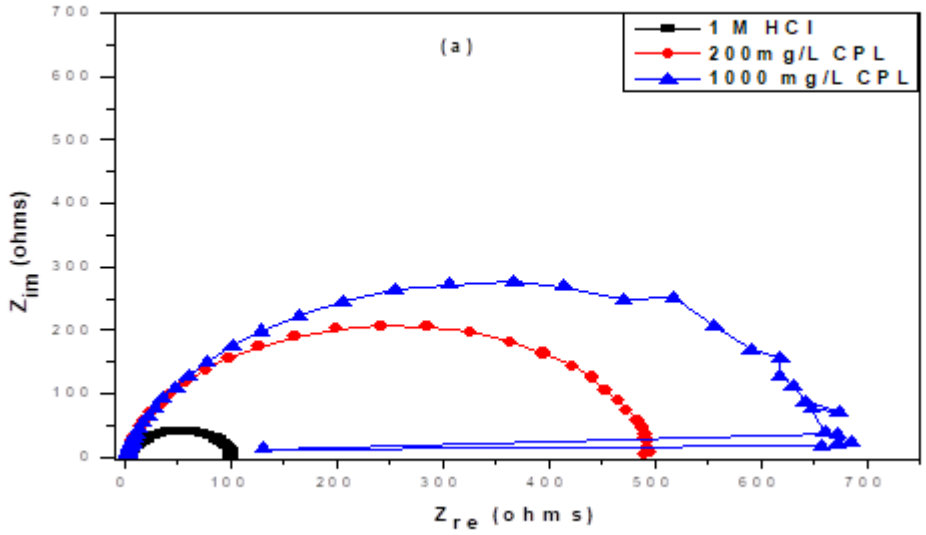

Figure 1: Electrochemical impedance spectroscopy for mild steel in.

3.1.1 Electrochemical impedance spectroscopy result of AL in the presence of CPL extract.

In the case of Al samples in 1M HCl and 0.5M H2SO4 solution, the Nyquist plots presented below show a capacitive loop then an inductive loop as illustrated in Fig 2. The diameter of the semicircles is correlated with the resistance to charge transfer. The capacitive loops on CPL were higher than when CPL was absent implying that Al corroded less in the presence of CPL. Both the aggressive solutions contain an inductive loop, which could be an indication of certain non-faradaic reactions at the sample/electrolyte interface, such as the adsorption of desorption of corrosion products. Based on Zsimpwin software, the impedances of Al in the two solutions were adjusted to the equivalent circuit model of Figure 3.

Rs is the solution resistance, Qdl and RLo are capacitance of charge and resistance of charge layer to penetration of electrolyte solution respectively. On the other hand, the inductance, L, and the charge transfer resistance, Rct, characterize the operations that take place under the charges storage. As per the findings, the Rpo was greater in case of the inhibited Al when compared to the uninhibited Al whereas, the Qpo was less in the inhibited environment as compared to the uninhibited solution. Similarly, the achieved inductance of the Al sample being inhibited was higher than the inductance of the uninhibited. This may indicate that addition of CPL will be able to modify the electrochemistry of the Al sample in that it will reduce the rate of corrosion in the acidic solutions by reducing the infiltration of electrolytes into the substrate electrolyte contact. This is further supported by the higher value of Rct of Al in the presence of the inhibitor as compared to the value realized in the absence of CPL.

It is common knowledge that as the Al surfaces get in contact with aqueous solutions, a layer of Al2O3 protection can be formed (Sastri et al, 2007). This layer may significantly decrease the electrochemical corrosion rate of the Al surface. However, it is in the presence of CPL that its species adsorbs on the Al surface leaving a strong barrier between the electrolyte solutions and the Al surface. Consequently, the corrosion potential of the Al sample shifts to more positive values (noble values) implying that there is less available electrochemical area on the sample. Also, the rate of penetration of the electrolyte is decreased by the inhibitor and consequently, the rate of electrochemical reactions between the Al/electrolyte interface is slowed down. Based on the obtained results, it appears that the exposure of the Al substrate to CPL reduces the susceptibility of the substrate to dissolution and the electrochemical processes that occur between the substrate and the electrolyte. This was shown by the shift of Ecorr to more positive potentials, the reduction in the density of the current in the inhibited environment and the increased width of the Nyquist plots. As it can be deduced, it is possible that the adsorption of CPL species serves as a shield to prevent the contact of the electrolyte solutions and the Al substrate (Kissi et al. 2006).

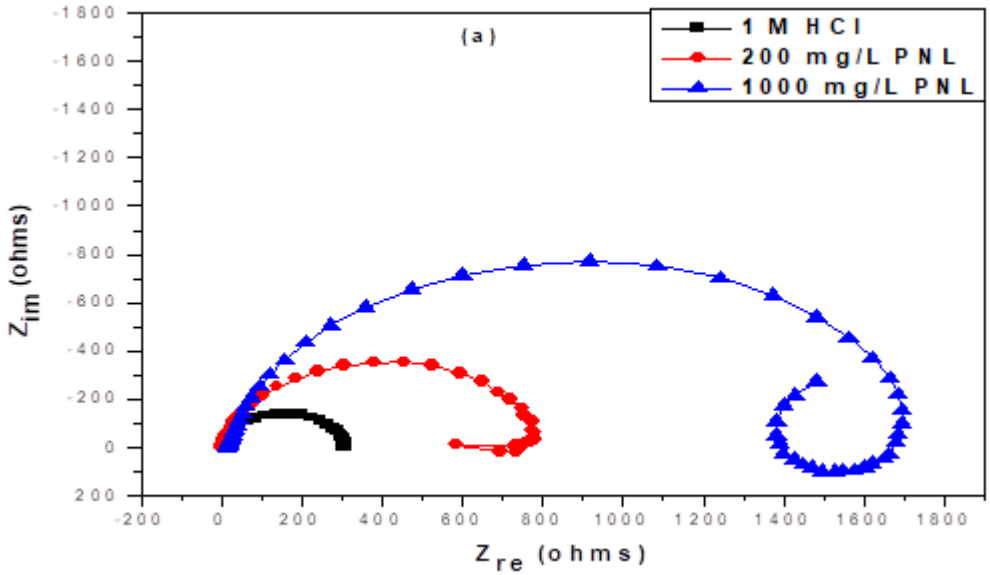

Figure 2: Impedance spectra of curves of Aluminium in: (a) 1 M HCl

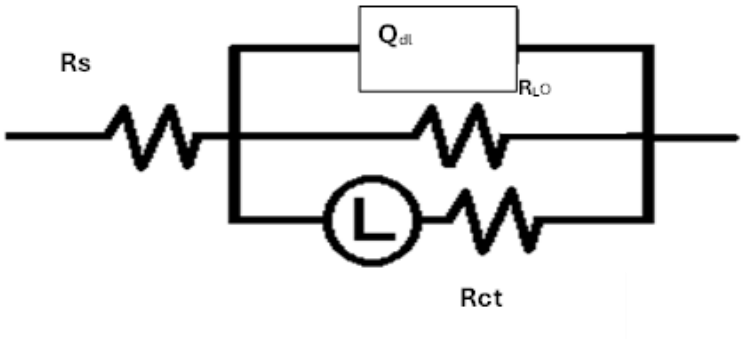

Figure 3: Equivalent Circuit Model for Al sample.

3.2 Result of Weight Loss Method using Response Surface Method (RSM)

Table 2 illustrates the response of weight loss, corrosion rate, and efficiency of an inhibitor to temperature, time, the concentration of an inhibitor, and the concentration of acids using carica papaya extract to inhibit the corrosion of aluminium, mild steel, and zinc in HCl and H2SO4.

Table 2: RSM Result of the Inhibition of Al in HCl Medium with CPL Extract

Std	Run	Factor 1, Acid Conc. (M)	Factor 2, Inhibitor Conc. (g/l)	Factor 3, Temperature (K)	Factor 4, Time (hr)	Response 1, Weight Loss (g)	Response 2, Corrosion Rate (mg/cm²hr)	Response 3, Inhibition Efficiency (%)
23	1	1	0.7	313	4	0.112	3.1	65.78
21	2	1	0.7	303	8	0.084	1.163	75.89
13	3	0.5	0.2	323	12	0.335	3.1	44.84
27	4	1	0.7	313	8	0.112	1.55	73.99
29	5	1	0.7	313	8	0.112	1.55	73.99
7	6	0.5	1.2	323	4	0.167	4.651	53.25
4	7	1.5	1.2	303	4	0.084	2.325	73.99
6	8	1.5	0.2	323	4	0.251	6.976	39.46
3	9	0.5	1.2	303	4	0.112	3.1	59.19
30	10	1	0.7	313	8	0.112	1.55	73.99
22	11	1	0.7	323	8	0.167	2.325	63.84
9	12	0.5	0.2	303	12	0.223	2.067	52.23
14	13	1.5	0.2	323	12	0.335	3.1	53.13
10	14	1.5	0.2	303	12	0.251	2.325	56.37
19	15	1	0.2	313	8	0.195	2.713	55.5
1	16	0.5	0.2	303	4	0.167	4.651	39.46
16	17	1.5	1.2	323	12	0.195	1.809	72.1
11	18	0.5	1.2	303	12	0.084	0.775	81.24
24	19	1	0.7	313	12	0.167	1.55	80.12
2	20	1.5	0.2	303	4	0.167	4.651	33.46
25	21	1	0.7	313	8	0.112	1.55	73.99
20	22	1	1.2	313	8	0.084	1.163	86.3
26	23	1	0.7	313	8	0.112	1.55	73.99
17	24	0.5	0.7	313	8	0.195	2.713	49.33
8	25	1.5	1.2	323	4	0.14	3.876	65.78
15	26	0.5	1.2	323	12	0.223	2.067	62.79
12	27	1.5	1.2	303	12	0.084	0.775	84.56
18	28	1.5	0.7	313	8	0.167	2.325	65.78
5	29	0.5	0.2	323	4	0.223	6.201	40.56
28	30	1	0.7	313	8	0.112	1.55	73.99

3.2.1 Analysis of variance (ANOVA) of the Inhibition Efficiency, IE (%).

in the ANOVA (analysis of variance). The significance of the model is shown by its F-value of 33.99. An F-value this high has a 0.01% probability of being caused by noise. Model terms are considered significant when "Prob > F" values are less than 0.0500. A, B, C, D, AB, BC, CD, and A^2 are important model terms in this instance. The model terms are not significant if the value is more than 0.1000. Model reduction may help your model if there are a lot of unnecessary model terms (not including those needed to maintain hierarchy). With a difference of less than 0.2, the "Pred R-Squared" of 0.8146 and the "Adj R-Squared" of 0.9409 are in acceptable agreement. "Adeq Precision" calculates the ratio of signal to noise. It is preferable to have a ratio larger than 4. A sufficient signal is shown by your ratio of 20.982. The design space may be traversed using this paradigm.

3.2.2 Models of the inhibition efficiency

The levels of forgiveness of the response of each element can be estimated based on the equation presented in the form of coded factors. The high and low values of the components are defaulted to the numbers +1 and -1 respectively. The coded equation can be applied to establish the relative effect of the factors by taking a comparison of the factor coefficients.

Corrosion Inhibition Efficiency Model Equation of CPL Extract in the Form of Coded Factors.

Inhibition Efficiency = +72.91+3.43* A+12.45* B-3.37* C+6.47+2.16+0.80* D* AB* AC+0.30* AD-2.60* BC-0.32* BD-2.16* CD-14.27* A^2-0.92* B^2-1.96* C^2+1.13* D^2 (13)

3.2.3 3D plots and diagnostic reports of Inhibition Efficiency, IE (%)

Three-dimensional maps of the viscosity of the corrosion inhibition are shown in figure 4. The interactions between the process factors in influencing the inhibition concentration were demonstrated in parabolic graphs. It was then established that there was a quadratic relationship between the answer and the variables taken into consideration (E.I. Ifediorah et al., 2025).

Figure 5 shows the predicted and actual versus run viscosities and residuals versus corrosion inhibition run of the RSM model that was fitted with the help of the polynomial equation.

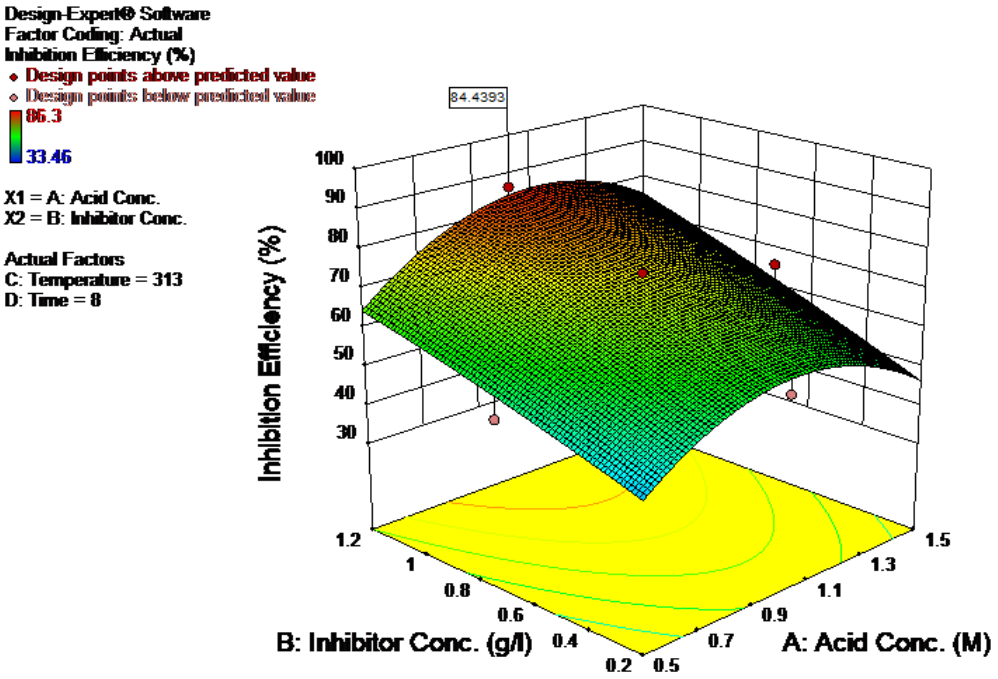

Figure 4: IE (%) of Al in HCl Medium with CPL Extract

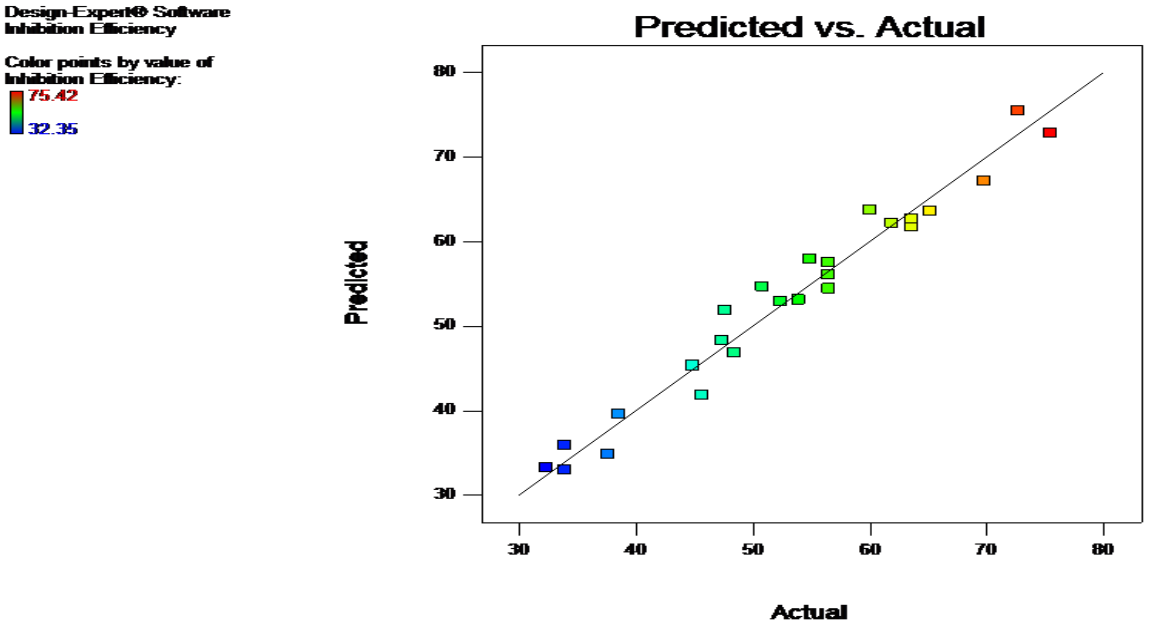

Figure 5: The predicted verses Actual viscosity of bio-hydraulic fluid

4. Conclusions

The constituents of Carica papaya (CPL), leaf extracts increase synergistic modes of inhibition to improve the overall efficiencies up to 89% via amplified surface passivation on aluminium, mild steel, and zinc under HCl/H2SO4 media. This synergy presents a electrochemical and gravimetric interaction, in which gravimetrically the blends decrease the rates of corrosion as verified by response surface methodology optimized weight loss data. Validation from gravimetric results (optimised through response surface methodology, RSM) was conducted through 3D plots, showing parabolic curve, which is typical for quadratic models. Combination of RSM to multivariate optimization (concentration, temperature, immersion time) and the responses. Electrochemical impedance spectroscopy (EIS) represents expanded Nyquist semicircles (Rct + to 520 Ohm cm2) and reduced double-layer capacitance (Cdl - to 32 muF cm -1), which can be ascribed to denser and cooperative film geometries. the molecular basis of these changes has been attributed to denser and cooperative film geometries, which in turn predict preferential adsorption sites and correlate (r = 0.95) with experimental inhibition capabilities, hence allowing DFT The theoretical-experimental synergy does not only confirm the physisorptive dominance (-14 kJ/mol, E a increases to 74 kJ/mol), but also provides the green engineering potentials, including the potential of adaptation inhibitors to dynamic industrial effluents or as a component of the intelligent coating with pH-responsive release. These plant-based extracts are the subject of recent systematic reviews as alternatives to toxic synthetics which incorporate alternative economically viable and biodegradable corrosion inhibitors that could reduce corrosion-related emissions by 2030 percent in such industries as petrochemicals and renewables.

References

Al-Moghrabi, A. A., Al-Abbas, F. M., and Al-Moghrabi, M. A., 2024. Plant extracts as green corrosion inhibitors for different kinds of steel. Heliyon, 10(15), Article e35092. https://doi.org/10.1016/j.heliyon.2024.e35092.

Bentiss, F., Gengembre, L., Lagrenée, M., Lebrini., M., and Vezin H., 2005. Electrochemical and quantum chemical studies of new thiadiazole derivatives adsorption on mild steel in normal hydrochloric acid medium. Corrosion Science 47, Pp. 485–505.

Bentiss, F., Lagrenée, M., Lebrini, M., Traisnel , M., and Vezin H., 2007. Experimental and theoretical study for corrosion inhibition of mild steel in normal hydrochloric acid solution by some new macrocyclic polyether compounds. Corrosion Science. 49, Pp. 2254–226.

Cerón, A., Cerón, L., and Cerón, M., 2018. Potential of using plant extracts as green corrosion inhibitors in the oil and gas industry. Croatian Journal of Food Science and Technology, 10(2), Pp. 95–102. https://doi.org/10.17508/cjfst.2018.10.2.95.

Chidiebere, M. A., Oguzie, E.E., Liu, L., Li, Y., Wang, F., 2014. Inhibitory action of Funtumia elastica extracts on the corrosion of Q235 mild steel in hydrochloric acid medium: experimental and theoretical studies, Journal of Dispersion Science and Technology.36, Pp. 8 - 16.

Chidiebere, M.A., Oguzie, E.E., Liu, L., Li, Y., Wang, F., 2014. Corrosion inhibition of Q235 mild steel in 0.5 M H_2SO_4 solution by phytic acid and synergistic iodide additives, Industrial and Engineering Chemistry Research,53, Pp. 7670 – 7679.

Dehghani, A., Bahlakeh, G., and Ramezanzadeh, M., 2024. Recent advances in green corrosion inhibitors from natural sources. Coordination Chemistry Reviews, 500, Article 215239. https://doi.org/10.1016/j.ccr.2023.215239.

E.I., Ifediorah, Mmonwuba N.C, Okolie L.E, Toochukwu K.T., and Ezeugo J.O. 2025. Formulation and Performance Evaluation of Sustainable Bio-Hydraulic Fluid from Spent Palm Kernel Oil Glycerin and Anacardium Occidentale Leaf Extract As a Corrosion Inhibitor. Journal of Engineering Research and Reports 27 (5): Pp. 443-62. https://doi.org/10.9734/jerr/2025/v27i51517.

Ifediorah E. I, A.K. Babayemi, O. L. Eluno, E. E. Eluno., 2025. Development and Evaluation of Biogrease from Biobased Oil Using Palm Bunch Lye, and Moringa Oleifera Leaf. Acta Chemica Malaysia, 9(1): Pp. 44-54.

Ifediorah E.I., Ezeugo J.O., 2025. Optimization and Experimental Evaluation of Bio-Hydraulic Fluid from Spent Palm Kernel Oil with Graphite, Eggshell, and Snail Shell Friction Modifiers. Acta Chemica Malaysia, 9(2): Pp. 104-110.

Ifediorah et al./ UNIZIK Journal of Engineering and Applied Sciences 5(1), Pp. 2345 – 2363.

Ifediorah, E. I., A. K. Babayemi, O. L. Eluno, and E. E. Eluno. 2025. Experimental Evaluation and RSM Optimization of Bio-Grease from Cottonseed Oil Using Sodium Hydroxide and Bio-Based Additives. Journal of Engineering Research and Reports 27 (5): Pp. 463-81. https://doi.org/10.9734/jerr/2025/v27i51518.

Koch, G., Varney, J., Thompson, N., Moghissi, O., Gould, M., and Payer, J., 2016. International measures of prevention, application, and economics of corrosion technologies study. NACE International.https://www.nace.org/resources/general-resources/corrosion-basics/economic-impact.

M. A. Chidiebere, E.E., Oguzie, L.Liu, Y.Li, F. Wang, 2015. Ascorbic acid as corrosion inhibitor for Q235 mild steel in acidic environments, Journal of Industrial and Engineering Chemistry Research, 25, Pp. 182 – 192

Martinez, S., and Stagljar, I., 2003. Correlation between the molecular structure and the corrosion inhibition efficiency of chestnut tannin in acidic solutions. Theochem. 640 Pp. 167 - 174.

Oghenerukevwe, P. O., Okpala, C. O., and Okoro, O., 2023. Carica papaya leaf extract (CPLE) as green corrosion inhibitor for AISI 4140 steel in 15% hydrochloric acid medium. Green Chemical Engineering, 4(4), Pp. 184–192. https://doi.org/10.1016/j.gce.2023.06.001.

Oguzie Emeka E, Chinonso B. Adindu, Conrad K. Enenebeaku, Cynthia E. Ogukwe, Maduabuchi A. Chidiebere and Kanayo L. Oguzie., 2012. Natural Products for Materials Protection: Mechanism of Corrosion Inhibition of Mild Steel by Acid Extracts of Piper guineense,58, Pp. 124-138.

Oguzie, E. E., Enenebeaku, C. K., Akalezi, C. O., Okoro, S. C., Ayuk, A. A., and Ejike, E. N., 2010. Adsorption and Corrosion inhibiting effect of Dacryodis edulis extract on low carbon steel corrosion in acidic media. Journal of Colloid Interface Science, 349, 283.

Okafor.P.C. and Ebenso.E.E., 2014. Inhibitive action of Carica papaya extracts on the corrosion of mild steel in acidic media and their adsorption characteristics. Pigment and Resin Technology (EMERALDINSIGHT, UK). 36(3): Pp. 134 – 140.

Olasehinde, E.F., Adesina, A.S. and Aderibigbe, A.D., 2012. Corrosion inhibition behaviour for mild steel by extracts of musa sapientum peels in HCl solution. Journal of Applied Chemistry, vol. 2, pp. 15 – 23.

Olszak, A., Nowak, A., and Kowalczyk, A., 2020. An overview of green corrosion inhibitors for sustainable and environment-friendly industrial development. Materials Today: Proceedings, 38, Pp. 193–198. https://doi.org/10.1016/j.matpr.2019.10.040.

Omotioma, M. and Onukwuli, O.D., 2015. Corrosion inhibition of mild steel in 1.0M HCl with castor oil extract as inhibitor. International Journal of Chemical Science, 14(1): Pp. 103-127.

Onen, A.I., 2010. Determination of the Amount of Corrosion of Iron using different Concentrations of two Alkali Halides with time, Yedzaram Journal of Science and Technology, 1 (1): Pp. 74-89.

Onen, A.I., 2011. Inhibition of Acid Corrosion of Mild Steel by Opuntia Spp (OSPP) Cactus Milk Extract, Nigerian Journal of Applied Sciences, 22: Pp. 174-181.

Onuchukwu, A. l., 2008. Electrochemical technology. Spectrum Books Ltd. Ibadan.P195.

Onuegbu, T.U., Umoh, E.T. and Ehiedu, C.N., 2013. Emilia sonclifolia extracts as green corrosion inhibitor for mild steel in acid media using weight loss method. Arabian Journal of Chemistry, Page 24-36.

Orubite, K.O. and Oforka, N.C., 2013. Inhibition of Corrosion of Mild Steel in HCl using Leaves Extract of Nypa Fruticans Wurmb, Material Letters, 58 (11): Pp. 1768.

Orwal., 2009. Agro forestry Data base; a tree reference and selection guide version 4.0 (http://www.worldagroforestry.org/sites/treedbs/treedatabase.asp)

Ozcan, M., Debri, I and Erbil, M., 2004. Organic Sulphur containing compounds as corrosion inhibitors for Mild Steel in Acidic Media: Correlation Between Inhibition Efficiency and Chemical Structure, Appl. Surf. Sci.Vol. 236, Pp.155-164.

R. T., 2025. Bitter leaf (Vernonia amygdalina) as a green corrosion inhibitor for protection of metals and alloys—A review. Journal of Materials and Environmental Sciences, 16(2), Pp. 015–028.

Rahim, A. A., and Rahim, A. A., 2023. Inhibitive effect of Carica papaya

leaves extract on the corrosion of mild steel in hydrochloric acid medium. Arabian Journal of Chemistry, 16(5), Article 104567. https://doi.org/10.1016/j.arabjc.2023.104567.

Rosliza, R.,Wannik, W.B and Sennin, H.B., 2008. Mater. Chem.P.107,281-288.

Safak, S., Duran, B., Yurt, A and Turkoglu, G., 2012, Corros.Sci. Vol. 54, Pp. 251.

Schmitt, G., and Bedbur, K., 1985. Investigations on structural and electronic effects in acid inhibitors by AC impedance. Werks. Korros., 36, Pp. 273 – 280.

Shreir, L.L., 2000. Basic Concepts of Corrosion. In: Corrosion, 3rd edition, Great Britain: Butterworth Heinemann.

Singh, A. and Singh, V.K., 2010. Inhibition effect of environmentally benign kuchla (strychnos nuxvomica) seed extract on corrosion of mild steel in HCL Solution. Rasayan Journal of Chemistry3(4) Pp. 811-824.

Singh, M.R., 2015. Litchi (Litchi Chinensis) peels extract as a potential green inhibitor in prevention of corrosion of mild steel in 0.5 M H_2SO_4 solution. Arbain Journal of Chemistry, Pp. 18 – 78.

U.S Department of Agriculture Forest Service., 2002. Rocky Mountain Research Station Fire Science Effect Information System. Available: http://www.fs.fed.us/database/feis/

U.S Department of agriculture, National Resources Conservation Service., 2001. The Plants Database, version 3.1 (http://plants.usda.gov) National Plant Data Center. Baton Rouge, LA70874 - 4490 USA.

Ugi, B.V. and Abeng, F.E., 2013. Corrosion inhibition effects and adsorption characteristics of ethanol extract of king's bitter root on mild steel in HCl and Tetraoxosulphate (vi) acid media. Journal of Natural and Applied Sciences 2(2): Pp. 10 – 21.

Umoren, S. A., and Solomon, M. M., 2019. Plant extracts as green corrosion inhibitors for different metal substrates in various corrosive media: A review. Processes, 7(12), Article 938. https://doi.org/10.3390/pr7120938Vashi.

Umoren, S. A; Obot, I. B and Obi-Egbedi, N. O., 2009. Raphia hookeri gum as a potential eco-friendly inhibitor for mild steel in sulfuric acid. J. Mater. Sci. Vol. 44. P. 274 - 279.

Umoren, S.A. Ogbobe, O.Ebenso,E.E.and Ekpe,U.J., 2012. Effect of halide ions on the corrosion inhibition of mild steel in acidic medium using polyvinyl alcohol. Pigment and Resin Technology (EMERALDINSIGHT, UK). 35 (5): Pp. 284 – 292.

Umoren, S.A. Ogbobe.O, and Ebenso,E.E., 2013. Synergistic Inhibition of aluminium corrosion in acidic medium by Gum Arabic and halide ions. Transactions of SAEST (CECRI, INDIA). 41(2): Pp. 74 – 81.

Umoren,S.A. Obot,I.A., Ebenso,E.E., Okafor,P.C., Ogbobe.O. and Oguzie,E.E., 2015. Gum Arabic as potential corrosion inhibitor for aluminium in alkaline medium and its adsorption characteristics. Anti- Corrosion Methods and Materials (EMERALDINSIGHT,UK). 53 (5): Pp. 277 – 282.

Umoren,S.A., Ogbobe.O. and Ebenso,E.E., 2014.The adsorption characteristics and synergistic inhibition between polyethylene glycol and halide ions on the corrosion of mild steel in acidic medium. Bulletin of Electrochemistry (CECRI, INDIA). 22 (4): Pp. 155 – 167.

Uppal, M.M. and Bhatia, S.C., 2001. Engineering Chemistry, 6th edition, Delhi: Khana Publishers.

Verma, C., Olasunkanmi, L. O., Akpan, I. B., Ebenso, E. E., and Quraishi, M. A., 2018. An overview on plant extracts as environmentally sustainable and green corrosion inhibitors for metals and alloys in aggressive corrosive media. Journal of Molecular Liquids, 266, Pp. 577–597. https://doi.org/10.1016/j.molliq.2018.06.095.

Yadav, P.N.S., 2010. Molecular Structure of Heterocyclic compounds and their Inhibitive Action for Corrosion of Grade 1100 Aluminium in dilute HCl, British Corrosion Journal, 34 (1): Pp. 51-56.